UC Irvine
UC Irvine Previously Published Works

Title

Visualizing Teixobactin Supramolecular Assemblies and Cell Wall Damage in B. Subtilis Using CryoEM

Permalink

Journal

ISSN

Authors

Hurst, Paul Joshua
Morris, Michael A
Graham, Annissa A
et al.

Publication Date

DOI

Peer reviewed

Visualizing Teixobactin Supramolecular Assemblies and Cell Wall Damage in *B. Subtilis* Using CryoEM

Paul Joshua Hurst, Michael A. Morris, Annissa A. Graham, James S. Nowick, and Joseph P. Patterson*
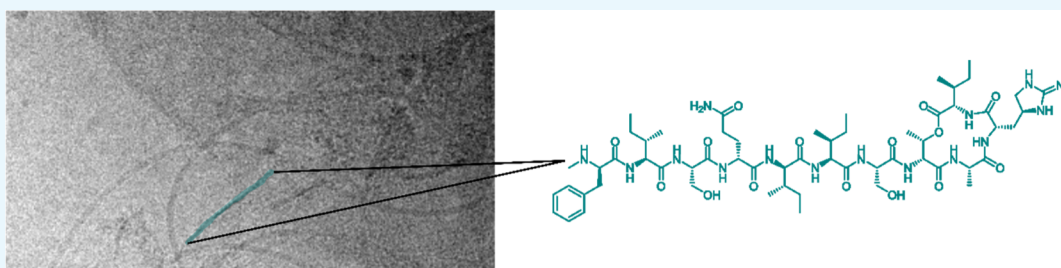
ACCESS | 📊 Metrics & More | 📖 Article Recommendations | 🆂🅸 Supporting Information

ABSTRACT: The antibiotic teixobactin targets bacterial cell walls. Previous research has proposed that the active form of teixobactin is a nano-/micron-sized supramolecular assembly. Here, we use cryogenic transmission electron microscopy to show that at 1 mg/mL, teixobactin forms sheet-like assemblies that selectively act upon the cell wall. At 4 μg/mL, teixobactin is active, and aggregates are formed either transiently or sparingly at the cell surface.

1. INTRODUCTION

The peptide antibiotic teixobactin was reported in 2015[1] and shows promise for addressing antibiotic resistance in Gram-positive bacteria.[1−7] The proposed mechanism of action is the inhibition of cell wall biosynthesis and peptidoglycan precursor recycling, leading to cellular lysis of bacteria.[1,2] Teixobactin targets the pyrophosphates of lipid II (peptidoglycan) and lipid III (teichoic acid) cell wall building blocks.[1,8] As these targets are extracellular and nearly immutable, it makes it difficult for bacteria to become resistant to teixobactin.[9]

To enable the design of antibiotics with improved pharmacological properties, several studies have tried to obtain a more detailed understanding of teixobactin's mechanism of action. Teixobactin has been shown to dimerize as a consequence of its stereochemical configuration and amphi-philicity.[1,10,11] The dimerization of teixobactin results in the formation of antiparallel β-sheets and higher order fibrils.[11] Solid-state nuclear magnetic resonance (NMR) studies of a teixobactin analogue in the presence of lipid II indicate that the N-terminal tail of teixobactin forms a β-sheet conformation that aggregates beyond the dimer state.[8] NMR spectroscopy and fluorescence microscopy studies of a teixobactin analogue in the presence of lipid II giant unilamellar vesicles (GUVs) showed the formation of micron-sized teixobactin-lipid II aggregates at the surface of the GUVs.[8,10] Fluorescence microscopy studies of a fluorescent teixobactin analogue in the presence of several Gram-positive bacteria, including *Bacillus subtilis*, corroborated that teixobactin binds to the cell walls of bacteria.[12] Collectively, these studies provide evidence that the active form of teixobactin and its analogues are nano-/micron-sized aggregates that form at the cell wall of bacteria.

To test this hypothesis, we performed cryogenic transmission electron microscopy (cryoEM) experiments on *B. subtilis* in the presence and absence of teixobactin. The advantage of cryoEM is that it can provide high-resolution images of the bacteria in a near-native state. This allows us to distinguish and inspect the features of bacteria, such as the cell wall, and how they respond to treatment with teixobactin. CryoEM also enables the visualization of the aggregation behavior of teixobactin at a nanoscale resolution. While most CryoEM antibiotic research focuses on the structural deduction of antibiotic interaction,[13−15] this study focuses on observing the presence of teixobactin aggregates and the effect teixobactin has on cellular features of *B. subtilis*.

2. RESULTS AND DISCUSSION

As a control, CryoEM experiments were performed on untreated *B. subtilis* [in phosphate-buffered saline (PBS) containing 5% dimethyl sulfoxide (DMSO)] to identify structural features of the cells in their native state (Figure 1).[16] *B. subtilis* was selected for this study due to its large size and its structural rigidity.[17] Suspensions of live *B. subtilis* were

Cell Membrane ↑
Cell Wall ↑
Bacterial Fibril ↑
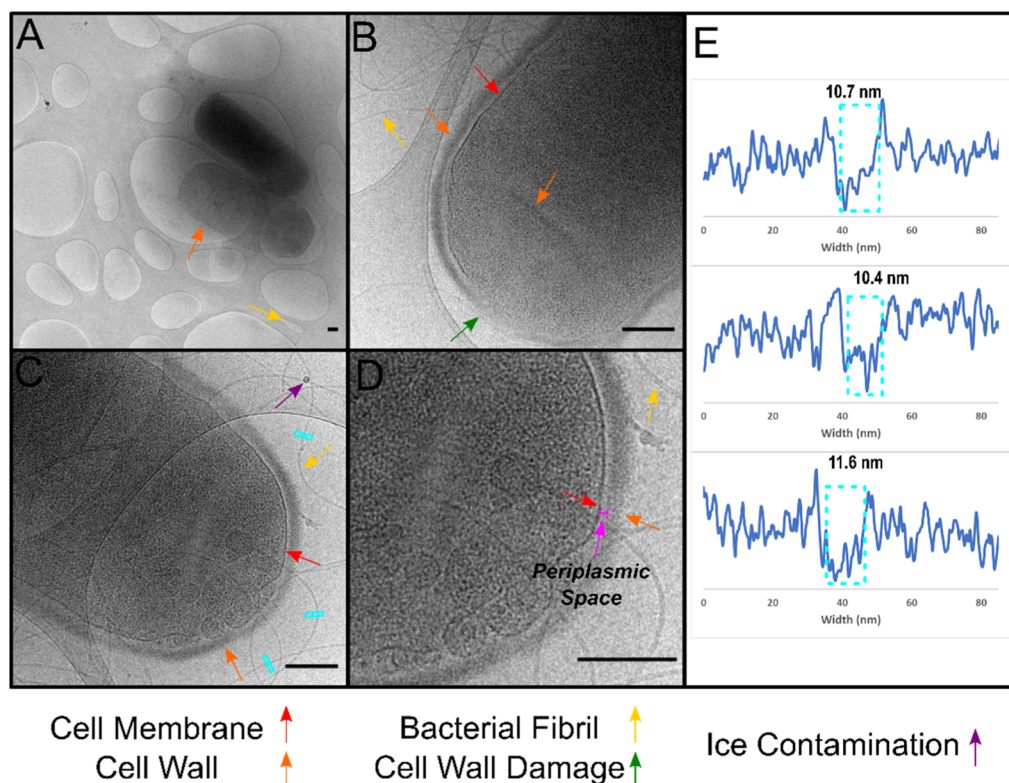Cell Wall Damage ↑
Ice Contamination ↑

Figure 1. CryoEM images of *B. subtilis* in PBS buffer and 5% DMSO. Scale bar is 200 nm. (A) Overview of the bacteria. (B,C) Images showing intra- and extracellular features such as the cell wall and bacterial fibrils. (D) Cropped region of the image in C highlighting the periplasmic space between the cell wall and cell membrane. (E) Line profiles from bacterial fibrils from the image in C (ordered from the top to the bottom); insets boxed in light blue.
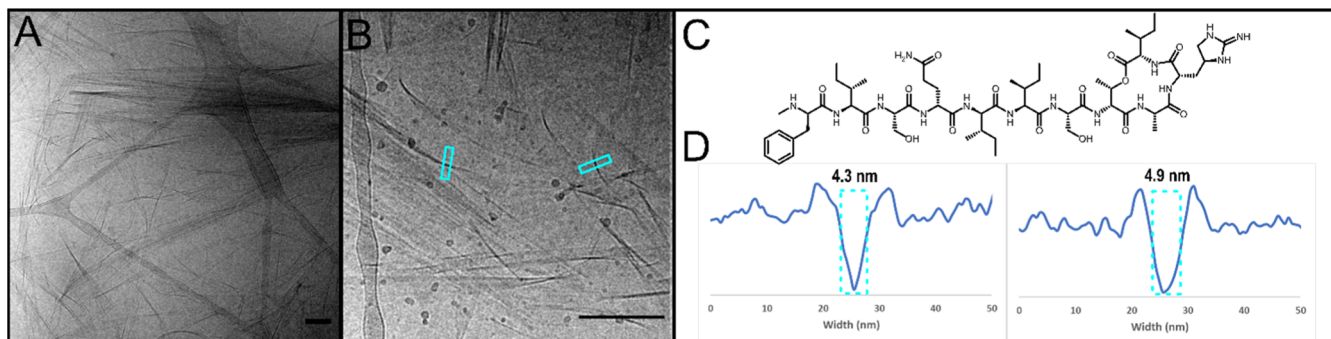

Figure 2. CryoEM images of 1 mg/mL teixobactin in PBS buffer and 5% DMSO. Scale bar is 200 nm. (A) Overview of teixobactin aggregates. (B) Teixobactin aggregates show the presence of sheet-like structures. (C) Molecular structure of teixobactin. (D) Line profiles measuring the thickness of sheets from B that are perpendicular to the imaging plane.

added to cryoEM grids, plunge-frozen, and imaged directly. In contrast to previous cryoEM studies on *B. subtilis*, we did not microtome or mill the cells with a focus-ion beam.[18−20] Consistent with the previous TEM studies on untreated *B. subtilis*, we were able to identify detailed intra- and extracellular features of *B. subtilis*, including vesicles, the cell membrane, cell wall, bacterial fibrils, and the periplasmic space (Figures 1, S1, and S2).[18−24] Bacterial cell walls were classified as being "intact" or "degraded". Degraded cell walls were then subclassified as containing a "low-density region", a "hole", or being "fully degraded". Details and examples of these classifications are given in Figures S3−S6 and Table S1. In the *B. subtilis* control sample, 19% of cells displayed cell wall degradation with 12% being low-density regions and 7% from the presence of a hole, and no cells were observed to be fully

degraded (*n* = 85). We believe that some of the observed cell wall degradation is related to natural processes that are a part of the bacterial life cycle. For example, sporulation is a process that results in cell wall degradation due to the release of a bacterial spore (see Figure 1B).[20,25] Cell wall or bacterial damage could also be the result of the shear forces exerted on the cells during the blotting stage of the cryoEM preparation.[26,27] Although we cannot identify the exact nature of each degraded cell wall, classification is important for comparison with that of *B. subtilis* treated with teixobactin. The *B. subtilis* control sample shows that bacterial fibrils were present in 86% of the micrographs. These fibrils are long and flexible with a diameter of 10.9 ± 0.8 nm (*n* = 55, Figure 1E and Table S2) and could be bacterial flagella or TasA protein fibrils. TasA protein fibrils are thought to be responsible for forming
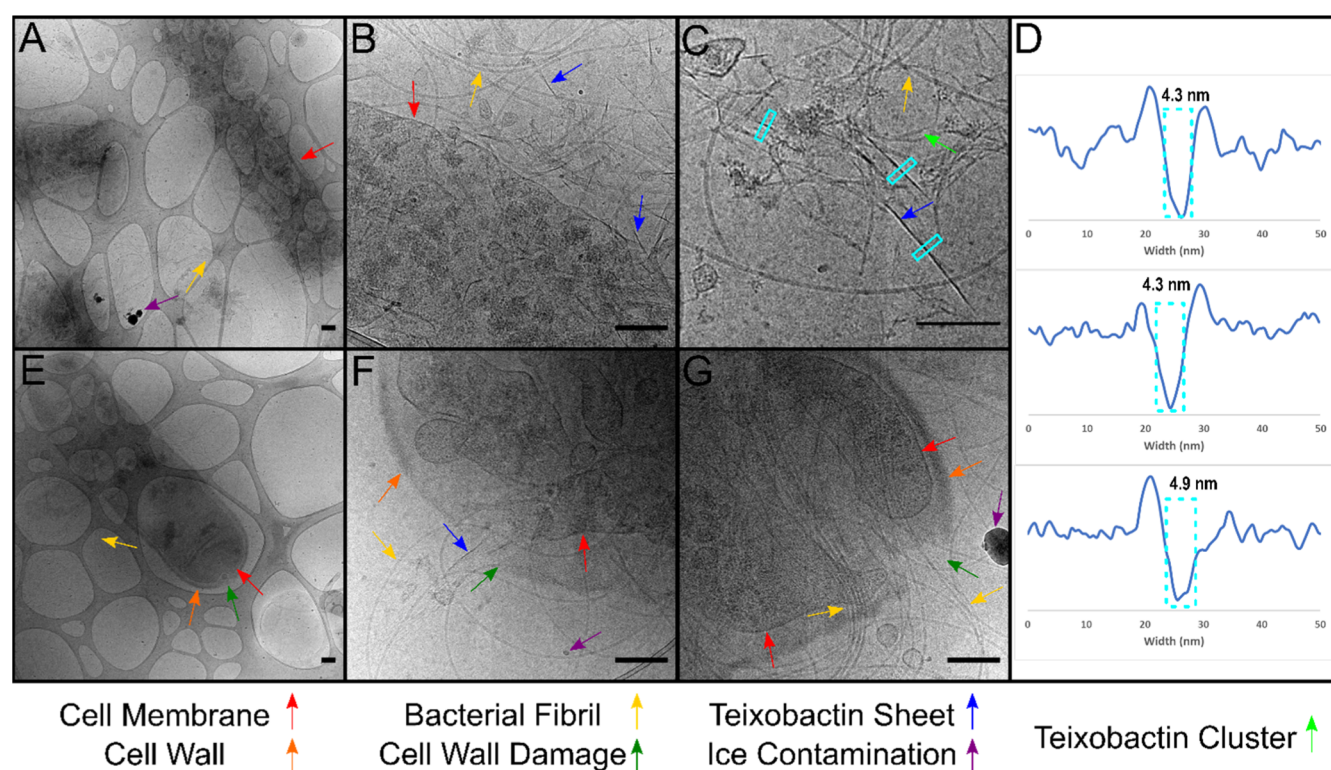
Figure 3. CryoEM images of *B. subtilis* treated with 1 mg/mL (A−D) and 4 µg/mL (E−G) teixobactin in PBS buffer and 5% DMSO. Scale bar is 200 nm. (A) Overview of the bacteria in the sample. Teixobactin aggregates are low-contrast and difficult to see at this magnification (B,C) Images showing low-contrast teixobactin clusters, higher-contrast teixobactin sheets, and bacterial remnants. (D) Line profile of teixobactin sheets measured in the image in C (the order is left to right). (E) Overview of the bacterium with cell wall damage. (F,G) Images showing cell wall damage in bacteria. Image F shows a possible teixobactin sheet.

biofilms.[24,28,29] Treatment with formic acid indicates that the fibrils are TasA (Figure S7).

As a second control, the aggregation behavior of teixobactin in solution, without *B. subtilis*, was studied by light scattering and cryoEM. Light scattering experiments were performed on a series of teixobactin solutions from 4 µg/mL to 1 mg/mL. The lower concentration is in line with the previous fluorescence microscopy studies of a fluorescent teixobactin analogue,[12] and the higher concentrations are in line with previous structural studies by solid-state NMR.[10] The light scattering results indicate a critical aggregation concentration of ∼0.2 mg/mL (Figure S8). CryoEM experiments on a 4 µg/mL teixobactin solution did not reveal any nano-/micron-sized aggregates (Figure S9). However, it should be noted that at such low concentrations, it would be difficult to find aggregates by cryoEM even if they were present. CryoEM experiments on the 1 mg/mL solution revealed that teixobactin forms nano-/micron-sized sheet-like structures (Figures 2 and S10). When the sheets are perpendicular to the imaging plane, they present as high-contrast "rod-like" structures, which enable the measurement of the sheet thickness to be 4.6 ± 0.9 nm (n = 216) (Table S3 and Figure S11). This thickness is similar to the diameter of the double helix of β-sheets formed by a Lys_{10}-teixobactin analogue.[11] The thickness and morphology of the teixobactin sheets are significantly different from those of the bacterial fibrils, making it easy to distinguish between them. It is important to note that the minimum inhibitory concentration (MIC) of teixobactin against *B. subtilis* is 0.06 µg/mL. Although these results show that there is no significant aggregation of teixobactin at low concentrations, aggregation in

the presence of bacteria could occur due to binding with the cell wall building blocks or a high local concentration at the bacterial surface.

To visualize interactions between *B. subtilis* and teixobactin using CryoEM, *B. subtilis* was treated with teixobactin at 1 mg/mL and 4 µg/mL. To optimize the imaging conditions for cryoEM, the concentration of bacteria used in our cultures was significantly increased compared to that in the MIC assay (2.4×10^8 CFU/mL compared to 5×10^5 CFU/mL),[1] and the bacteria were treated for 4 h, compared to 16 h for the MIC assay. Therefore, it is reasonable to expect that only a fraction of the bacteria will be dead upon sampling. The purpose of the high-concentration experiments is to determine if we can identify teixobactin aggregates at the surface of *B. subtilis*, if the structure of the teixobactin aggregates changes due to the presence of *B. subtilis*, and what structural effects the teixobactin aggregates have on the cell wall. CryoEM experiments at 1 mg/mL (Figures 3A−D and S12) showed that 100% of the cells had cell wall damage. 96% of cells displayed complete degradation, and 4% displayed a hole (n = 146). Interestingly, many bacteria display an intact cell membrane, even though the cell wall has been completely degraded, indicating the formation of a protoplast.[30] This indicates that teixobactin has a specificity toward the cell wall and supports the hypothesis that teixobactin aggregates play a role in the destruction of the cell walls of Gram-positive bacteria. The cryoEM images show the presence of teixobactin sheets, which are most easily identified when oriented perpendicular to the imaging plane (Figure 3C,D). The sheet structures have a thickness of 4.5 ± 0.7 nm (n = 128),

consistent with the measurements in teixobactin samples prepared in the absence of bacteria. The cryoEM images also show the presence of clusters composed of rod-/fiber-like structures which are structurally distinct from both the teixobactin and bacterial fibrils with a diameter of 7.2 ± 0.7 nm ($n = 67$) (Figures 3C and S13 for the histogram). Considering that these clusters are not observed in either control sample, we believe that they are the result of teixobactin binding to cell wall precursors, consistent with previous reports.[8,10]

CryoEM images of the 4 μg/mL (Figures 3E−G and S14) sample showed that 69% of cells had cell wall degradation. 6% contained low density regions, 53% contained holes, and 10% displayed complete degradation ($n = 169$). This shows that teixobactin is active in this sample, as evidenced by the increase in cell wall degradation compared to that in the control, and that we can image both predegradation and postdegradation cells. Despite imaging 169 cells, only six sheet-like structures were found (6%, $n = 104$), and we found no evidence of the cluster structures (Figure S15). Additional experiments at 4 μg/mL using 0.2% DMSO showed little to no sheet-like structures (3% of 75 images and 0% of 58 images), and no cluster structures were found. The sheets had an average thickness of 4.8 ± 0.6 nm, which is consistent with the teixobactin control. In only one case, a sheet is spatially correlated with a cell wall hole (Figure 3F). This could be seen as evidence to support the hypothesis that the active form of teixobactin is an aggregated state. However, we believe that the observation is inconsistent with the frequency of cell wall degradation. Furthermore, based on the previous fluorescence microscopy studies, we would expect to see aggregates present around all of the bacterial cells.[12] There are two possible interpretations of this data. (1) The majority of the teixobactin molecules do not form nano-/micron-sized aggregates at the surface of the bacteria and are in a nonaggregated state. (2) Most teixobactin molecules form nano-/micron-sized aggregates at the bacterial surface, but they form transiently and disassemble after acting upon the cell wall. It is important to note that the "nonaggregated states" we are referring to here could include teixobactin dimers or higher-order oligomers which would be too small to be observed under these imaging conditions. In both interpretations, teixobactin is present at the surface of the bacteria in both the nano-/micron-sized aggregated state and nonaggregated state. This mixture of species makes it difficult to conclude if one or both species are active upon the cell wall. Another interesting observation is that the bacterial fibrils seem unaffected by teixobactin. The average diameters and abundance were consistent across all samples (Table S3). Although bacterial fibrils have been hypothesized to provide some antibacterial resistance, our data indicate that teixobactin does not degrade or interact with the fibrils.

3. CONCLUSIONS

In summary, cryoEM data show that at concentrations of ~1 mg/mL, teixobactin forms sheets and clusters in the presence of *B. subtilis*, which correlates with cell wall degradation. At 4 μg/mL, teixobactin is still active upon the cell wall, but teixobactin aggregates are only found in 6% of micrographs. One possible interpretation of the data is that at low concentrations, the aggregates form transiently, making their observation by cryoEM challenging. Collectively, the data support the hypothesis that teixobactin acts upon the cell

wall[8,10,12] and provide evidence that teixobactin is present in both the aggregated and nonaggregated states. Further studies are required to determine if aggregation is a prerequisite for activity. This study also shows that cryoEM can provide important information regarding the aggregation behavior of antibiotics in the presence of cells.

4. MATERIALS AND METHODS

Culturing Bacteria for Imaging. *B. subtilis* (ATCC 6051) was cultured overnight (ca. 16 h) in Mueller−Hinton broth in a shaking incubator at 37 °C. The following morning, the cultures were diluted 1:100 in Mueller−Hinton broth and were allowed to grow exponentially in a shaking incubator (225 rpm) at 37 °C. Once an OD_{600} of ca. 0.3 was achieved, 500 μL of bacteria was transferred to a sterile Eppendorf tube, and the bacteria were centrifuged at 4000 rpm (1300g) for 5 min.

Treatment with Teixobactin. While the bacteria were being centrifuged, 1 mg/mL and 4 μg/mL solutions of teixobactin [HCl salt, NovoBiotic Pharmaceuticals, characterized by high-performance liquid chromatography (HPLC) and matrix-assisted laser desorption ionization (MALDI) Figures S16−S18] were freshly prepared. The 1 mg/mL teixobactin solution was prepared by diluting 50 μL of the 20 mg/mL DMSO stock solution of teixobactin in 950 μL of sterile PBS. The 4 μg/mL teixobactin solution was prepared by combining 4 μL of the 1 mg/mL DMSO stock solution of teixobactin and 46 μL of sterile DMSO so that the final concentration of DMSO in the solution was 5%. To this solution, 950 μL of sterile PBS was then added to create a 4 μg/mL teixobactin solution. After centrifuging the bacteria (see above), the supernatant was removed, the pellet was resuspended in 500 μL of either 1 mg/mL or 4 μg/mL teixobactin solution or 5% v/v DMSO in sterile DMSO as a control, and the bacteria were incubated in a shaking incubator (225 rpm) at 37 °C for 4 h. The samples were then prepared for CryoEM analysis.

Light Scattering. Measurements were taken with a Malvern Zetasizer ZS Nano dynamic light scattering instrument. For each sample, the instrument was set to automatic runs (ranging from 10 to 20) to ensure that the instrument achieved a sufficient signal, and averages of three measurements were taken. The data displayed poor fit to the autocorrelation function, which is typical for highly anisotropic samples with broad size distributions (lengths and widths of the sheets). Consequently, we plotted the derived count rate to look for changes in the total scattering.

Cryogenic Transmission Electron Microscopy. CryoEM samples were prepared from bacterial solutions within less than 1 hour after sample preparation onto Lacey Carbon or Quantifoil R2/2 (Electron Microscopy Sciences) grids. Grids were glow-discharged for 70 s to increase the hydrophilicity prior to sample loading. Vitrification was carried out by an Automatic Plunge Freeze ME GP2 (Leica Microsystems) with 3 μL of the sample. Grid preparation was performed at 95−99% humidity, and the grids were blotted for 3 s prior to plunging into liquid propane. CryoEM samples were then placed on a Gatan CryoEM holder and imaged on a JEOL 2100 transmission electron microscope using a Schottky-type field-emission gun operating at 200 keV. Images were recorded using Serial EM software with a Gatan OneView CMOS camera at 4 × 4 k resolution. Additional CryoEM samples of this study are provided in Figures S19 and S20. Image measurements were performed on a Digital

Micrograph (Gatan) by creating line profiles, and the half-width minimum of intensity peaks was measured.

ASSOCIATED CONTENT

ⓈⒾ Supporting Information

The Supporting Information is available free of charge at https://pubs.acs.org/doi/10.1021/acsomega.1c04331.

Quantified cryoEM data, additional cryoEM images of *B. subtilis*, cryoEM images of cell wall classifications, light scattering data (derived count rate) of teixobactin solutions, additional cryoEM images of teixobactin solutions, additional cryoEM images of *B. subtilis* treated with teixobactin, histogram of all measured species in the 1 mg/mL teixobactin *B. subtilis* sample, cryoEM insets of sheet-like structures in the 4 μg/mL teixobactin *B. subtilis* sample, HPLC and MALDI characterizations of teixobactin, and additional cryoEM images from additional samples (PDF)

AUTHOR INFORMATION

Corresponding Author

Joseph P. Patterson − *Department of Chemistry, University of California—Irvine, Irvine, California 92697-2025, United States; Department of Materials Science and Engineering, University of California, Irvine, California 92697, United States;* ⓞ orcid.org/0000-0002-1975-1854; Email: patters3@uci.edu

Authors

Paul Joshua Hurst − *Department of Chemistry, University of California—Irvine, Irvine, California 92697-2025, United States;* ⓞ orcid.org/0000-0002-1826-2549

Michael A. Morris − *Department of Chemistry, University of California—Irvine, Irvine, California 92697-2025, United States;* ⓞ orcid.org/0000-0003-4526-271X

Annissa A. Graham − *Department of Chemistry, University of California—Irvine, Irvine, California 92697-2025, United States*

James S. Nowick − *Department of Chemistry, University of California—Irvine, Irvine, California 92697-2025, United States;* ⓞ orcid.org/0000-0002-2273-1029

Complete contact information is available at:
https://pubs.acs.org/10.1021/acsomega.1c04331

Notes

The authors declare no competing financial interest.

ACKNOWLEDGMENTS

REFERENCES

(1) Ling, L. L.; Schneider, T.; Peoples, A. J.; Spoering, A. L.; Engels, I.; Conlon, B. P.; Mueller, A.; Schäberle, T. F.; Hughes, D. E.; Epstein, S.; Jones, M.; Lazarides, L.; Steadman, V. A.; Cohen, D. R.; Felix, C. R.; Fetterman, K. A.; Millett, W. P.; Nitti, A. G.; Zullo, A. M.; Chen, C.; Lewis, K. A new antibiotic kills pathogens without detectable resistance. *Nature* **2015**, *517*, 455−459.

(2) Homma, T.; Nuxoll, A.; Gandt, A. B.; Ebner, P.; Engels, I.; Schneider, T.; Götz, F.; Lewis, K.; Conlon, B. P. Dual Targeting of Cell Wall Precursors by Teixobactin Leads to Cell Lysis. *Antimicrob. Agents Chemother.* **2016**, *60*, 6510−6517.

(3) Abdel Monaim, S. A. H.; Jad, Y. E.; El-Faham, A.; de la Torre, B. G.; Albericio, F. Teixobactin as a scaffold for unlimited new antimicrobial peptides: SAR study. *Bioorg. Med. Chem.* **2018**, *26*, 2788−2796.

(4) Yang, H.; Chen, K. H.; Nowick, J. S. Elucidation of the Teixobactin Pharmacophore. *ACS Chem. Biol.* **2016**, *11*, 1823−1826.

(5) Wen, P.-C.; Vanegas, J. M.; Rempe, S. B.; Tajkhorshid, E. Probing key elements of teixobactin−lipid II interactions in membranes. *Chem. Sci.* **2018**, *9*, 6997−7008.

(6) Karas, J. A.; Chen, F.; Schneider-Futschik, E. K.; Kang, Z.; Hussein, M.; Swarbrick, J.; Hoyer, D.; Giltrap, A. M.; Payne, R. J.; Li, J.; Velkov, T. Synthesis and structure−activity relationships of teixobactin. *Ann. N.Y. Acad. Sci.* **2020**, *1459*, 86−105.

(7) Gunjal, V. B.; Thakare, R.; Chopra, S.; Reddy, D. S. Teixobactin: A Paving Stone toward a New Class of Antibiotics? *J. Med. Chem.* **2020**, *63*, 12171−12195.

(8) Shukla, R.; Medeiros-Silva, J.; Parmar, A.; Vermeulen, B. J. A.; Das, S.; Paioni, A. L.; Jekhmane, S.; Lorent, J.; Bonvin, A. M. J. J.; Baldus, M.; Lelli, M.; Veldhuizen, E. J. A.; Breukink, E.; Singh, I.; Weingarth, M. Mode of action of teixobactins in cellular membranes. *Nat. Commun.* **2020**, *11*, 2848.

(9) Lloyd, D. G.; Schofield, B. J.; Goddard, M. R.; Taylor, E. J. De Novo Resistance to Arg10-Teixobactin Occurs Slowly and Is Costly. *Antimicrob. Agents Chemother.* **2020**, *65*, e01152−20.

(10) Öster, C.; Walkowiak, G. P.; Hughes, D. E.; Spoering, A. L.; Peoples, A. J.; Catherwood, A. C.; Tod, J. A.; Lloyd, A. J.; Herrmann, T.; Lewis, K.; Dowson, C. G.; Lewandowski, J. R. Structural studies suggest aggregation as one of the modes of action for teixobactin. *Chem. Sci.* **2018**, *9*, 8850−8859.

(11) Yang, H.; Du Bois, D. R.; Ziller, J. W.; Nowick, J. S. X-ray crystallographic structure of a teixobactin analogue reveals key interactions of the teixobactin pharmacophore. *Chem. Commun.* **2017**, *53*, 2772−2775.

(12) Morris, M. A.; Malek, M.; Hashemian, M. H.; Nguyen, B. T.; Manuse, S.; Lewis, K.; Nowick, J. S. A Fluorescent Teixobactin Analogue. *ACS Chem. Biol.* **2020**, *15*, 1222−1231.

(13) Tegunov, D.; Xue, L.; Dienemann, C.; Cramer, P.; Mahamid, J. Multi-particle cryo-EM refinement with M visualizes ribosome-antibiotic complex at 3.5 Å in cells. *Nat. Methods* **2021**, *18*, 186−193.

(14) Su, W.; Kumar, V.; Ding, Y.; Ero, R.; Serra, A.; Lee, B. S. T.; Wong, A. S. W.; Shi, J.; Sze, S. K.; Yang, L.; Gao, Y.-G. Ribosome protection by antibiotic resistance ATP-binding cassette protein. *Proc. Natl. Acad. Sci. U.S.A.* **2018**, *115*, 5157−5162.

(15) Crowe-McAuliffe, C.; Graf, M.; Huter, P.; Takada, H.; Abdelshahid, M.; Nováček, J.; Murina, V.; Atkinson, G. C.; Hauryliuk, V.; Wilson, D. N. Structural basis for antibiotic resistance mediated by the Bacillus subtilis ABCF ATPase VmlR. *Proc. Natl. Acad. Sci. U.S.A.* **2018**, *115*, 8978−8983.

(16) Because the teixobactin stock solution concentration is 20 mg/mL in DMSO, a dilution to 1 mg/mL, which is used in this study, is 5% DMSO. Therefore, to ensure that the sample matrix was identical in all samples, all samples in the paper were run with 5% DMSO in a PBS buffer.

(17) Pasquina-Lemonche, L.; Burns, J.; Turner, R. D.; Kumar, S.; Tank, R.; Mullin, N.; Wilson, J. S.; Chakrabarti, B.; Bullough, P. A.; Foster, S. J.; Hobbs, J. K. The architecture of the Gram-positive bacterial cell wall. *Nature* **2020**, *582*, 294−297.

(18) Matias, V. R. F.; Beveridge, T. J. Cryo-electron microscopy reveals native polymeric cell wall structure in Bacillus subtilis 168 and the existence of a periplasmic space. *Mol. Microbiol.* **2005**, *56*, 240−251.

(19) Matias, V. R. F.; Beveridge, T. J. Lipoteichoic Acid Is a Major Component of the Bacillus subtilis Periplasm. *J. Bacteriol.* **2008**, *190*, 7414.

(20) Khanna, K.; Lopez-Garrido, J.; Zhao, Z.; Watanabe, R.; Yuan, Y.; Sugie, J.; Pogliano, K.; Villa, E. The molecular architecture of engulfment during Bacillus subtilis sporulation. *eLife* **2019**, *8*, No. e45257.

(21) Brown, L.; Kessler, A.; Cabezas-Sanchez, P.; Luque-Garcia, J. L.; Casadevall, A. Extracellular vesicles produced by the Gram-positive bacterium Bacillus subtilis are disrupted by the lipopeptide surfactin. *Mol. Microbiol.* **2014**, *93*, 183−198.

(22) Liu, B.; Qiao, H.; Huang, L.; Buchenauer, H.; Han, Q.; Kang, Z.; Gong, Y. Biological control of take-all in wheat by endophytic Bacillus subtilis E1R-j and potential mode of action. *Biol. Contr.* **2009**, *49*, 277−285.

(23) Liu, H.; Pei, H.; Han, Z.; Feng, G.; Li, D. The antimicrobial effects and synergistic antibacterial mechanism of the combination of ε-Polylysine and nisin against Bacillus subtilis. *Food Contr.* **2015**, *47*, 444−450.

(24) Romero, D.; Aguilar, C.; Losick, R.; Kolter, R. Amyloid fibers provide structural integrity to Bacillus subtilis biofilms. *Proc. Natl. Acad. Sci. U.S.A.* **2010**, *107*, 2230−2234.

(25) Stephens, C. Bacterial sporulation: A question of commitment? *Curr. Biol.* **1998**, *8*, R45−R48.

(26) Zheng, Y.; Lin, Z.; Zakin, J. L.; Talmon, Y.; Davis, H. T.; Scriven, L. E. Cryo-TEM Imaging the Flow-Induced Transition from Vesicles to Threadlike Micelles. *J. Phys. Chem. B* **2000**, *104*, 5263−5271.

(27) Glaeser, R. M. Preparing Better Samples for Cryo−Electron Microscopy: Biochemical Challenges Do not End with Isolation and Purification. *Annu. Rev. Biochem.* **2021**, *90*, 451.

(28) Huang, J.; Liu, S.; Zhang, C.; Wang, X.; Pu, J.; Ba, F.; Xue, S.; Ye, H.; Zhao, T.; Li, K.; Wang, Y.; Zhang, J.; Wang, L.; Fan, C.; Lu, T. K.; Zhong, C. Programmable and printable Bacillus subtilis biofilms as engineered living materials. *Nat. Chem. Biol.* **2019**, *15*, 34−41.

(29) Branda, S. S.; Chu, F.; Kearns, D. B.; Losick, R.; Kolter, R. A major protein component of the Bacillus subtilis biofilm matrix. *Mol. Microbiol.* **2006**, *59*, 1229−1238.

(30) Cushnie, T. P. T.; O'Driscoll, N. H.; Lamb, A. J. Morphological and ultrastructural changes in bacterial cells as an indicator of antibacterial mechanism of action. *Cell. Mol. Life Sci.* **2016**, *73*, 4471−4492.